Geophysical Research Letters

RESEARCH LETTER
10.1029/2018GL081295

Key Points:
- 3-D thermo-mechanical modeling was performed to investigate the impact of the arrival of a mantle plume below a subducting lithospheric plate
- The thermal and buoyancy effects of a mantle plume prove sufficient to induce the separation of a microcontinent from the subducting plate
- The proposed scenario is consistent with a separation of the Apulian microcontinent from Africa during subduction of the Neo-Tethys

Supporting Information:
- Supporting Information S1

Correspondence to:
A. Koptev,
alexander.koptev@ifg.uni-tuebingen.de

Citation:
Koptev, A., Beniest, A., Gerya, T., Ehlers, T. A., Jolivet, L., & Leroy, S. (2019). Plume-induced breakup of a subducting plate: Microcontinent formation without cessation of the subduction process. *Geophysical Research Letters*, *46*, 3663–3675. https://doi.org/10.1029/2018GL081295

Received 12 NOV 2018
Accepted 20 MAR 2019
Accepted article online 25 MAR 2019
Published online 2 APR 2019

Plume-Induced Breakup of a Subducting Plate: Microcontinent Formation Without Cessation of the Subduction Process

Alexander Koptev[1,2], Anouk Beniest[3], Taras Gerya[4], Todd A. Ehlers[1], Laurent Jolivet[2], and Sylvie Leroy[2]

[1]Department of Geosciences, University of Tübingen, Tübingen, Germany, [2]Institut des Sciences de la Terre de Paris (ISTeP), Sorbonne Université, CNRS, Paris, France, [3]Department of Earth Sciences, Vrije Universiteit Amsterdam, Amsterdam, The Netherlands, [4]ETH-Zurich, Institute of Geophysics, Zurich, Switzerland

Abstract Separation of microcontinents is explained by a ridge jump toward the passive margin as a possible consequence of plume-induced rheological weakening, ultimately leading to breakup followed by accretion of the oceanic crust along a new spreading center. In contrast to such a purely extensional case, the separation of continental microblocks from the main body of the African plate during its continuous northward motion and subduction under Eurasia is still poorly understood. Our numerical experiments show the thermal and buoyancy effects of mantle plume impingement on the bottom of the continental part of a subducting plate are sufficient to induce separation of an isolated microcontinental block from the main subducting continent, even during induced plate motion necessary for uninterrupted oceanic and continental subduction. Subsequent continental accretion occurs by decoupling upper-crustal nappes from the newly formed subducting microcontinent, which is in agreement with the Late Cretaceous-Eocene evolution of the eastern Mediterranean.

Plain Language Summary Separation of microcontinental blocks from their parent continent is usually attributed to abrupt relocation of concentrated extension from the mid-oceanic ridge to the adjacent continental margin. In the context of extensional passive margin evolution, previous extensive numerical and analog studies have revealed that hot upwelling mantle flow plays a key role in the mechanical weakening of the passive margin lithosphere needed to initiate a ridge jump. This, in turn, results in continental breakup and subsequent microcontinent isolation. However, the consequences of mantle plume impingement on the base of a moving lithospheric plate that is already involved into subduction are still unexplored quantitatively. Here we present the results of 3-D thermo-mechanical models showing that even in the context of induced plate motion (contractional boundary conditions), which are necessary to sustain continuous convergence, thermal and buoyancy effects of the mantle plume emplaced at the bottom of the continental part of the subducting plate are sufficient to initiate continental breakup and the subsequent opening of a new oceanic basin that separates the microcontinental block from the main body of the continent. With these models, we show that it is physically possible to form microcontinents in a convergent setting without the cessation of subduction.

1. Introduction

Microcontinents are defined as independent blocks of continental lithosphere that are isolated from any other continental domains and are surrounded by ocean floor (Peron-Pinvidic & Manatschal, 2010; Scrutton, 1976). Jan Mayen in the Norwegian-Greenland Sea (Blischke et al., 2016; Gudlaugsson et al., 1988; Myhre et al., 1984; Peron-Pinvidic et al., 2012; Schiffer et al., 2018), the Seychelles in the Indian Ocean (Collier et al., 2009; Dickin et al., 1986; Ganerød et al., 2011; Plummer & Belle, 1995), and the East Tasman Plateau and the Gilbert Seamount Complex in the Tasman Sea (Exon et al., 1997; Gaina et al., 1998, 2003) are usually cited as "typical" examples of separated microcontinental blocks (Figure 1a) as they are formed in a purely extensional tectonic setting. The best example of such microcontinents is the Jan Mayen platform separated from East Greenland in the Oligocene-Early Miocene due to a ridge jump toward the passive continental margin with the cessation of spreading at the existing mid-oceanic ridge (Gaina et al., 2009; Lundin & Doré, 2002). In this and certain other cases, rerifting and subsequent breakup along a passive margin is triggered by the thermal effect of an arriving mantle plume. The increase in temperature causes a

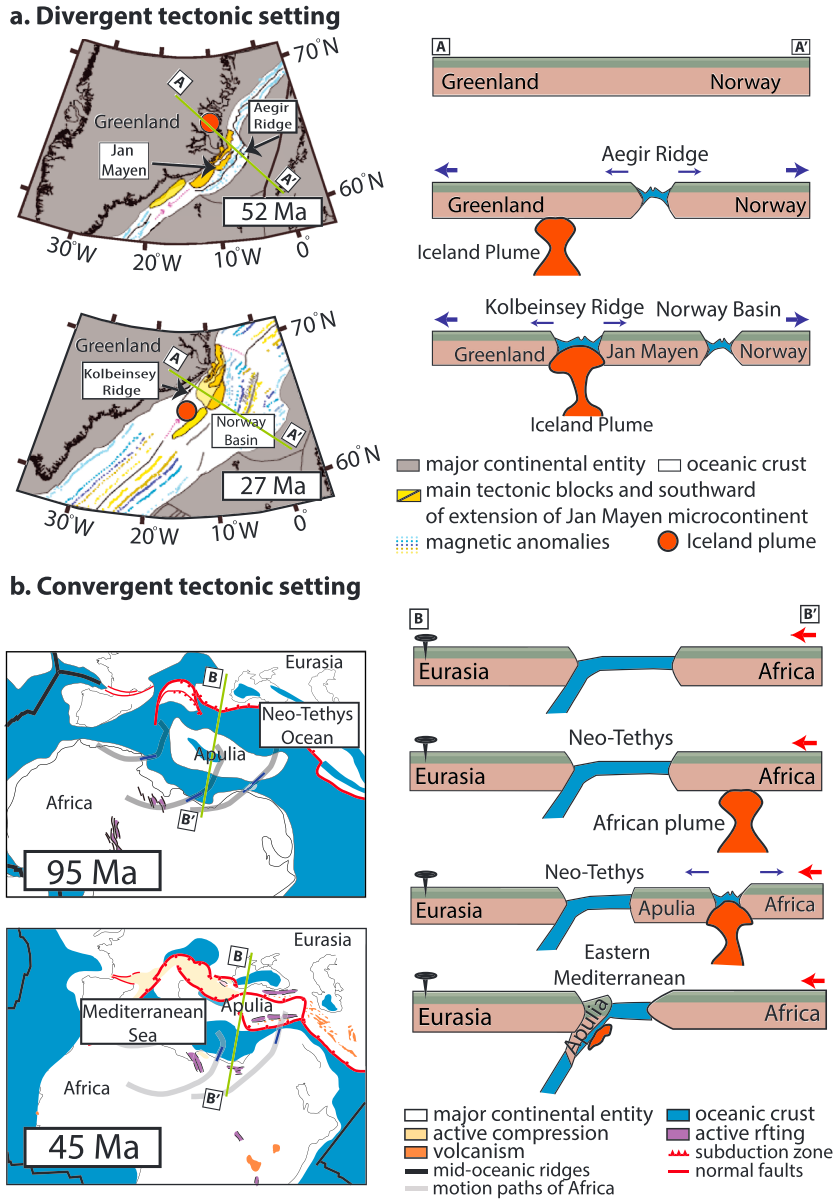

Figure 1. Plate reconstructions and schematic scenarios illustrating two principal types of the microcontinents: (a) microcontinent formed in a purely extensional tectonic setting: the North Atlantic region, separation of the Jan Mayen microcontinent from East Greenland (reconstruction after Torsvik et al., 2015); (b) microcontinent formed in the context of continuous convergence of the plates: Africa and the Neo-Tethys ocean, the Apulian microcontinent detached from Africa and then accreted to the Eurasia during ongoing subduction of the Neo-Tethys lithosphere. The layer colors on the schematic profiles correspond to the rock types shown on Figure 2.

decrease in the strength of the lithosphere that is large enough to relocalize the extension center from the mid-oceanic ridge toward the inner flank of the continental margin (Müller et al., 2001, and references therein). Apart from a severe weakening due to plume-induced reheating, intrinsic differences in lithospheric strength between different parts of the passive margin (Molnar et al., 2018; Vink et al., 1984) and plate reorganization events (Whittaker et al., 2016) have also been considered to influence the segregation of continental fragments.

Another group of microcontinents refers to microblocks that are detached from the continental segment of lithosphere during continuous subduction of its oceanic counterpart under the active margin of the opposite continent (Figure 1b). Natural examples have been found in the eastern Mediterranean, where an intricate

assemblage of tectonic units implies that several continental fragments were successively separated from Africa and then accreted to the Eurasian margin (Barrier et al., 2018; Barrier & Vrielynck, 2008; Dercourt et al., 1986; Menant et al., 2016; Sengör & Yilmaz, 1981), while the Neo-Tethys was consumed by subduction (Agard et al., 2011; Dercourt et al., 1993; Hafkenscheid et al., 2006; Jolivet et al., 2016; Takin, 1972). In particular, the Apulian microcontinent detached from Africa in the Jurassic (Frizon de Lamotte et al., 2011; Jolivet et al., 2016; Ricou, 1994) and drifted away from Africa to subduct and collide with Eurasia in the Late Cretaceous-Eocene resulting in the building of the Taurides in the east and the Hellenides in the west (Dercourt et al., 1986; Jolivet et al., 2003; Van Hinsbergen et al., 2005). Later, in the Late Eocene-Early Oligocene, continental rifting started in the Red Sea and Gulf of Aden (Ghebreab, 1998; Leroy et al., 2012; Roger et al., 1989; Watchorn et al., 1998), which ultimately led to Africa-Arabia breakup in the Early Miocene (Bosworth et al., 2005; Joffe & Garfunkel, 1987; Leroy et al., 2010; Mohriak & Leroy, 2013). In contrast to the Apulian microcontinent, Arabia separated from Africa at the very last stage of the Neo-Tethys during Africa/Arabia-Eurasia collision (Bellahsen et al., 2003; Jolivet & Faccenna, 2000; Koptev, Gerya, et al., 2018). The northern Appalachians (e.g., Van Staal et al., 2009, 2012) and southern Alaska (e.g., Bruhn et al., 2004; Enkelmann et al., 2017; Plafker & Berg, 1994) are other classical examples of complex mountain belts formed by accretion of tectonic terranes during the Early to Middle Paleozoic and in the Cretaceous-Cenozoic, respectively.

Over the last decade, several numerical studies have been performed to investigate the origin of microcontinents in extensional settings. Possible mechanisms for intraoceanic ridge-jumps (d'Acremont et al., 2010; Mittelstaedt et al., 2008, 2011) and for mid-oceanic ridge jumps to the passive continental margins have been explored by both numerical (Beniest, Koptev & Burov, 2017; Beniest, Koptev, Leroy, et al., 2017; Lavecchia et al., 2017) and analog (Dubinin et al., 2018) modeling studies. However, it is still not apparent how microcontinents form in a convergent tectonic system like Africa during its motion toward Eurasia. Part of the enigmatic nature of these microcontinents is the overall contractional tectonic regime in which diverging forces act locally to separate slivers of continental lithosphere from the main body. Such extensional episodes resulting in the stripping of the microcontinents have been attributed to the push of mantle plumes periodically arriving at the base of the African lithosphere (Faccenna et al., 2013; Jolivet et al., 2016). These mantle plume events and associated large igneous provinces of the past 180–300 Myr (Burke et al., 2008; Ernst, 2014; Jourdan et al., 2008; Torsvik et al., 2006) are related to a long-lived thermal upwelling through the mantle beneath Africa (Forte & Mitrovica, 2001) that is often referred as "African Superplume" (Gurnis et al., 2000). It likely emanates from a large-scale, low seismic velocity province at the core-mantle boundary (Ritsema et al., 1999). The recent numerical models show that the mantle superplumes might be a result of an upwelling return flow in response to deeply subducting slabs penetrating the lower mantle (Dal Zilio, 2018; Dal Zilio et al., 2018; Heron et al., 2015; Zhang et al., 2010).

However, the exact consequences of the arrival of the ascending mantle plume at the base of the continental part of the subducting lithospheric plate on microcontinents separation and their subsequent subduction and/or accretion at the opposite continental margin have never been estimated quantitatively and thus remain in many aspects unclear.

Here we present the results of a 3-D high-resolution thermo-mechanical model that investigates the effect of mantle plume impingement on the base of an already moving subducting continental lithospheric plate that contains an oceanic domain continuously sinking below the opposite continent. With these experiments we test the hypothesis that the buoyancy and thermal influence of a mantle plume are sufficient to induce separation and isolation of microcontinental blocks even in the context of uninterrupted plates' convergence.

2. Numerical Model Description

We produced the simulations presented in this contribution using the viscous-plastic code "I3ELVIS" (see supporting information and Gerya & Yuen, 2007, and Gerya, 2010, for more details).

The model domain (Figure 2) measures 1,000 × 400 × 200 km in the x, y, and z dimensions. This model box is resolved by 501 × 201 × 101 grid points thus offering a spatial resolution of ca. 2 km per grid cell in each direction.

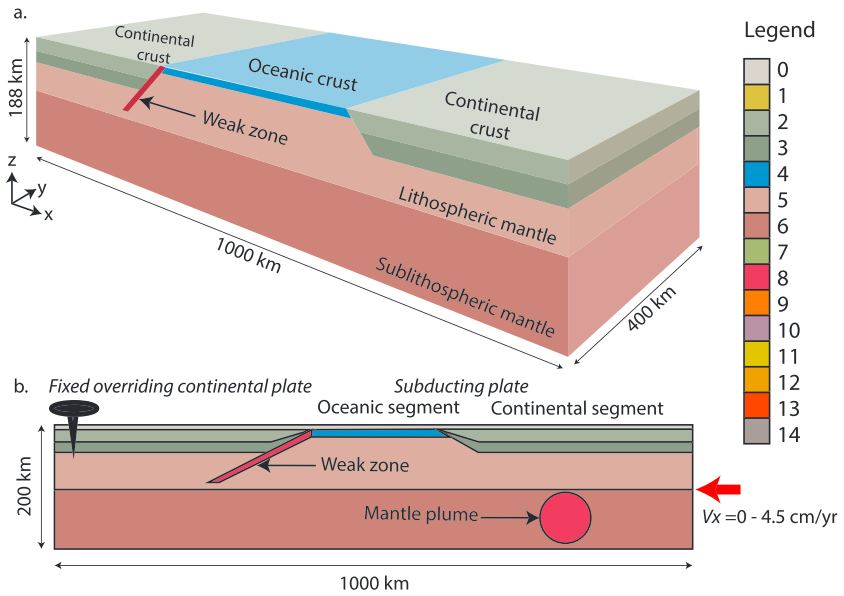

Figure 2. Initial model setup: (a) the 3-D view; (b) the vertical cross-section. The model domain consists of an overriding continental lithosphere and subducting lithospheric plate including both oceanic and continental lilithosphere. A mantle plume (40-km radius thermal anomaly of 1900–2000 °C) is seeded underneath the continental part of subducting plate. A weak zone characterized by low plastic strength and wet olivine rheology has been implemented in order to provide a rheological decoupling between the upper and subducting plate, enabling subduction of the incoming oceanic lithosphere beneath the overriding continent (e.g., Burg & Gerya, 2005; Vogt et al., 2017, 2018; Willingshofer et al., 2013). The top surface of the lithosphere is defined as an internal free surface through a 12-km-thick layer of "sticky air" (Crameri et al., 2012; Duretz et al., 2011; Gerya, 2010). The code "I3ELVIS" accounts for mineralogical phase changes by thermodynamic solution for density, obtained from the optimization of Gibbs free energy for a typical mineralogical composition of the lithospheric/sublithospheric mantle and plume material (Connolly, 2005). Partial melting is implemented using the most common parameterization (Gerya, 2013; Katz et al., 2003) of hydrous mantle melting processes. The color legend for different types of the rocks includes the following: 0 = sticky air; 1 = sediments; 2 = upper continental crust; 3 = lower continental crust; 4 = oceanic crust/underplated mafic material; 5 = lithospheric mantle; 6 = sublithospheric mantle; 7 = hydrated continental crust; 8 = hydrated mantle/mantle plume; 9 = melt-bearing continental crust; 10 = melt-bearing gabbro; 11 = melt-bearing lithospheric mantle; 12 = melt-bearing sublithospheric mantle; 13 = melt-bearing hydrated mantle/mantle plume; 14 = quenched mantle. Hydrated, partially molten and quenched rocks not shown on Figure 2 will appear over the evolution of the experiments (see Figures 3–5).

The initial model setup consists of two parts: (1) an overriding continental lithosphere (400 km wide) and (2) a subducting slab that includes both oceanic and continental lithospheric segments (200 and 400 km wide). The continental crust consists of 20 km of felsic (wet quartzite ductile flow law) upper crust and 15 km of mafic (plagioclase flow law) lower crust. The oceanic crust is represented by 8 km of basalt and gabbroic rocks (plagioclase flow law). Both the lithospheric and the sublithospheric mantle are composed of anhydrous peridotite (dry olivine flow law).

The velocity boundary conditions are free slip at both the front and back sides of the model box ($y = 0$ km and $y = 400$ km). The right boundary ($x = 1{,}000$ km) uses a uniform and constant-in-time x-parallel velocity (varied from 0 to 4.5 cm/year), which defines the material influx. The left boundary ($x = 0$ km) is fixed, meaning zero displacement in all directions. Mass conservation is ensured by the material outflux through the upper and lower permeable boundaries ($z = 0$ and $z = 200$ km).

The laterally uniform thermal structure of the continents is piece-wise linear with 0 °C at the surface (i.e., at the boundary between sticky air and upper crust) and 1,350 °C at 100 km ("normal" continental geotherm) or 90 km depth ("elevated" continental geotherm). The initial thermal distribution in the oceanic lithosphere is defined by a half-space cooling age at 60 Ma (Turcotte & Schubert, 2002). Both continental and oceanic lithospheres overlay a sublithospheric mantle with an initial adiabatic temperature gradient of ~0.5 °C/km.

We start our modeling procedure with the "no plume" model **1** (see Table S1), including a normal continental geotherm (1350 °C isotherm at 100 km depth) in both the overriding and subducting plates and a

horizontal material influx at the right model side (*Vx*) of 4.5 cm/year. Next, we introduce in this setup a mantle plume anomaly below the subducting continent. This anomaly is characterized by different initial temperatures—normal (1900 °C, model **2**) and relatively "high" (2000 °C, model **3**). Finally, we test the impact of an elevated continental geotherm (1350 °C isotherm at 90 km) with the experiments characterized by a normal (1900 °C) plume temperature and different boundary velocities of material influx (*Vx*) varying from 4.5 cm/year (model **4**) through 3.0 cm/year (model **5**), 1.5 cm/year (model **6**) and 0.3 cm/year (model **7**) to 0 cm/year (model **8**). Note that in these experiments (model **4**–**8**), the elevated continental geotherm is only applied to the subducting plate while the continental lithosphere of the overriding plate keeps the normal thermal gradient.

3. Results

In the no plume experiment (model **1**, Figure 3a), subduction of the oceanic lithosphere is followed by sinking of the continental part of the subducting plate. Initiation of the continental subduction coincides in time (~5 Myr) with the onset of partial melting of the hydrated mantle material composing the initial "weak zone" seeded between the overriding and subducting plates. At a later stage of the system's development (~10 Myr), the subducted continent reaches depths of 100 km where its upper crust is also involved in melting. Similar temporal transitions of subduction-related magmatism from mafic with mantle origin to felsic with crustal origin geochemical signature are reported in the Malayer-Boroujerd plutonic complex in western Iran (Deevsalar et al., 2018).

In the remaining experiments (models **2**–**8**; Figures 3b–3d, 4, and 5), the mantle plume seeded by a temperature anomaly at the bottom of the model box ascents quickly (~0.1 Myr) to the base of the continental part of the overlying plate. The thermal impact of the upwelling hot mantle leads to partial melting of not only the plume itself but also of adjacent lithospheric and sublithospheric material. For the models with the normal temperature gradient (models **2**–**3**), this mixed melt is attached to the bottom of the lithosphere and moves together with the plate into the subduction zone (Figures 3b and 3c) without a strong influence on the system's evolution compared to that of the no plume model **1** (Figure 3a). Note, however, that model **3** with a relatively "hot" thermal anomaly (initial temperature of 2000 °C) shows a deeper penetration of the plume into the lithospheric mantle and a more intense percolation of melts that are continuously generated from the melt-bearing material, thereby resulting in the underplating of mafic magmas at the crust-mantle boundary (Figure 3c).

An increase of the continental geotherm leads to large changes in the system's behavior (models **4**–**8** with elevated thermal gradient; Figures 3d, 4, 5, S1, and S2). Mantle plume impingement on the bottom of the lithosphere (Figure S1a) is followed by fast (~25 cm/year) penetration of hot plume material through the mantle (Figure S1b). This leads to thinning of the continental lithosphere and decompressional melting of both lithospheric and asthenospheric mantle in the area of plume emplacement and along the spontaneously localizing trench-parallel rifting zone that crosses the entire model domain (Figures 4a and S2b). This spontaneous rifting characterized by a quick transition in time from wide to narrow mode (Figure S2a and S2b) likely results from the presence of intraplate extensional stresses produced by both the plume-induced divergence and the growing pulling force of the continuously subducting oceanic slab. These extensional stresses result in a rapid and focused continental breakup in less than 0.5 Myr after the model's onset (Figure 4b). Note that the breakup first occurs in the central part of the model domain (i.e., above the plume apex) while in the peripheral segments the transition from the pre-breakup rifting to post-break spreading is delayed by ~0.2–0.3 Myr (Figures S1c and S2c). This breakup leads to the separation of the newly formed microcontinent from the main continental body of the subducting plate (Figure 4c).

The combined effect of the plume push and pulling force of a negatively buoyant slab results in a lateral displacement of the separated microblock that is considerably faster (~10–15 cm/year) than the imposed boundary condition velocity (~4.5 cm/year) at the right side of the subducting plate (Figure S3). Therefore, despite this continuous external push, a trench-parallel oceanic basin opens within a few Myr (Figures S2d) reaching a width of ~100 km wide above the plume impingement point (Figure S1d).

The sensitivity analysis of the previous results with different boundary conditions (models **5**–**8**) shows that fast plume-induced continental breakup occurs within 0.5 Myr in all experiments, regardless the magnitude of the applied external push (Figure 5). In contrast, the maximum width of the newly formed ocean basin

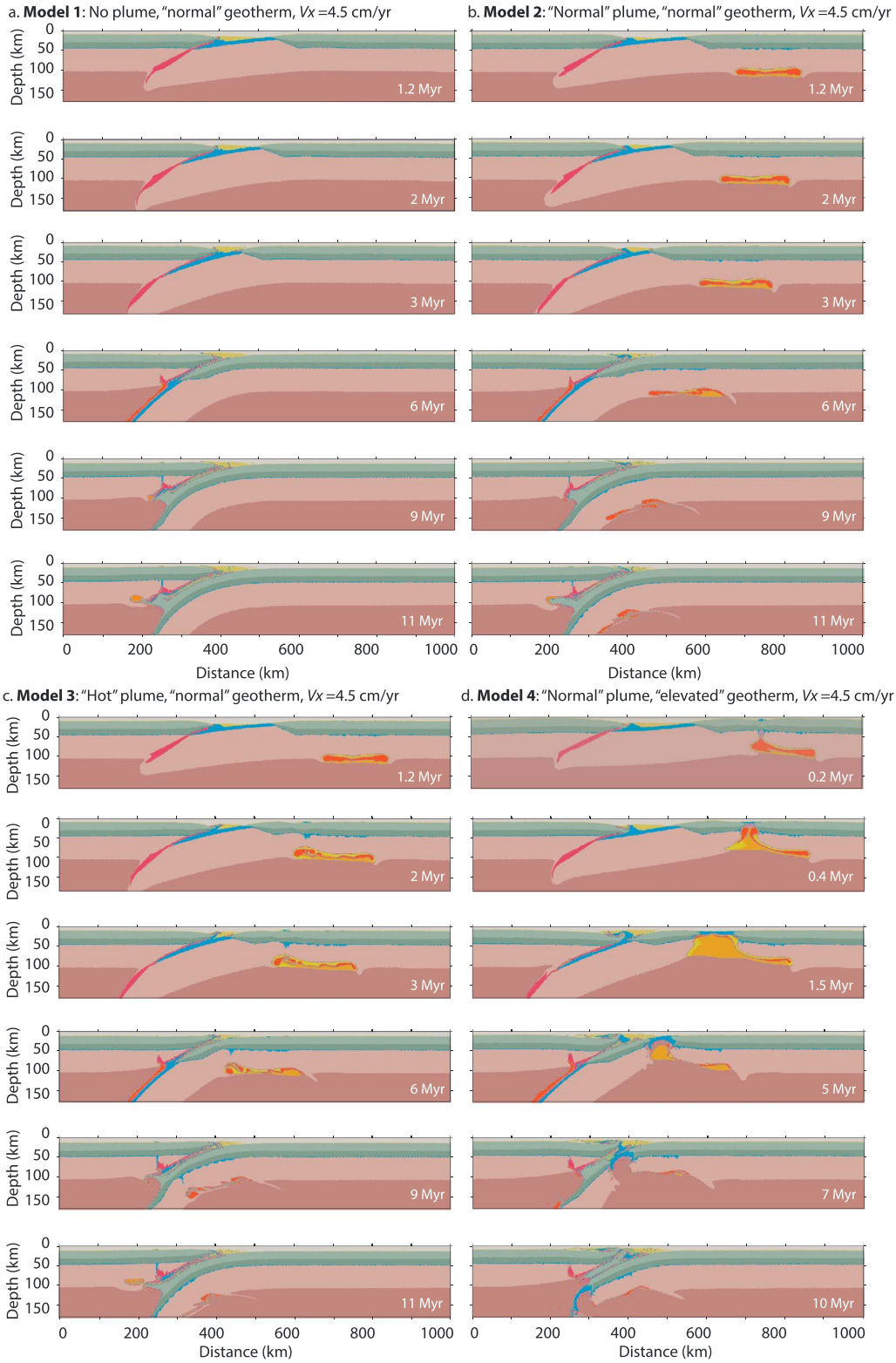

Figure 3. Central vertical cross-sections showing the evolution over time for the following experiments: (a) model **1**, no plume; (b) model **2**, mantle plume of "normal" temperature (1900 °C); (c) model **3**, "hot" mantle plume (2000 °C); (d) model **4**, "elevated" continental geotherm (1350 °C isotherm at 90 km) above normal (1900 °C) mantle plume. All these experiments are characterized by the same velocity of horizontal influx: $Vx = 4.5$ cm/year. Colors of rock types are as on Figure 2.

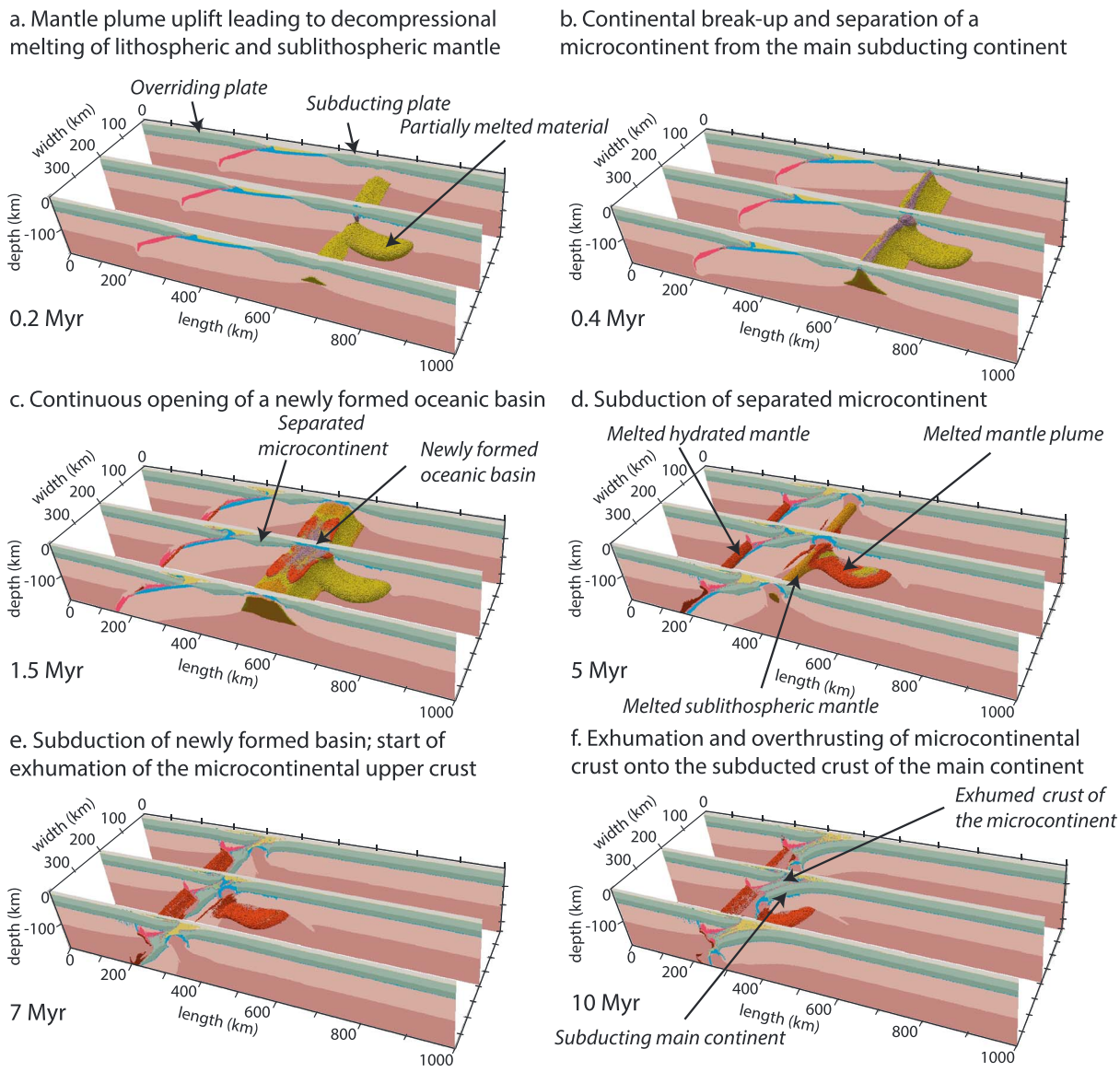

Figure 4. (a–f) The 3-D view of the temporal evolution for the model **4** ("elevated" continental geotherm above "normal" mantle plume, Vx = 4.5 cm/year; see Table S1). Colors of rock types are as on Figure 2.

varies as a function of the boundary velocities: it increases from 100 to 200 km as the external push decreases from 3.0 to 0 cm/year (Figure 5).

As soon as the initial ocean is completely subducted, the separated microcontinental block starts to sink below the overriding continental plate (Figure 4d). After having reached its maximum depth (~100 km), buoyant upper crust of subducting microcontinent decouples from the lower crust and mantle and migrates upward to the surface in a return flow along the subduction channel (Figures 4e and 4f). The fluid-saturated oceanic crust of the newly formed basin, which is also involved in the subduction, may play a lubricating role in this exhumation process. Note that more advanced exhumation occurs in the central segment of the model domain (Figure 4f) possibly due to the thermal impact of the mantle plume. A comparison of the model sensitivity to different boundary velocities of material influx (models **4**–**7**) shows that faster subduction leads to an earlier onset of exhumation of the upper microcontinental crust. The time of exhumation initiation varies from 7–9 Myr through 12 Myr to 45 Myr with a decrease of applied push (Vx) from 4.5–3.0 cm/year through 1.5 to 0.3 cm/year (see Figures 3d, 4e, and 5a–5c). Note also that in the case of relatively "fast" subduction (models **4**–**5**; Vx = 4.5–3.0 cm/year), exhumation of the microcontinental upper

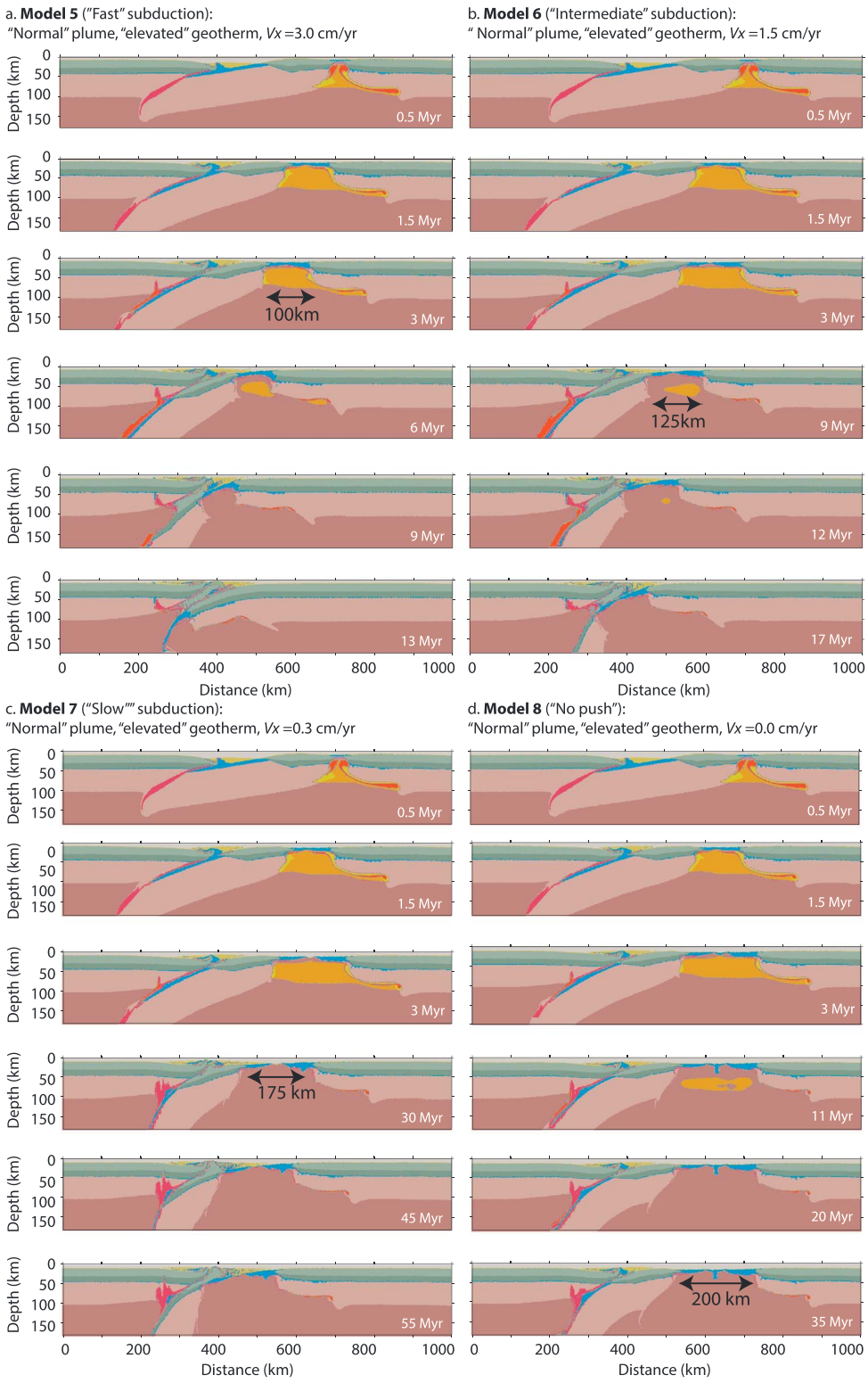

Figure 5. Central vertical cross-sections showing the evolution for the experiments characterized by normal temperature of the mantle plume (1900 °C), "elevated" continental geotherm (1350 °C isotherm at 90 km) in the overriding plate and varied velocities of horizontal influx at the right model boundary: (a) model **5**, *Vx* = 3.0 cm/year; (b) model **6**, *Vx* = 1.5 cm/year; (c) model **7**, *Vx* = 0.3 cm/year; (d) model **8**, *Vx* = 0.0 cm/year. Note a gradual increase of the maximum width of newly formed oceanic basin from 100 km through 125–175 km to 200 km with decreasing *Vx* from 3.0 cm/year through 1.5–0.3 to 0 cm/year. Colors of rock types are as on Figure 2.

crust occurs simultaneously with the subduction of the main continent. As a result, exhumed microcontinental crust overthrusts the crust of the subducted main continent while newly formed oceanic crust is deeply (>100 km) subducted (Figures 3d, 4f, and 5a). This is different for the "intermediate" case (model **6**, $Vx = 1.5$ cm/year) where the exhumed crust of the microcontinent is underlain by oceanic material of the new basin because the exhumation process was already ongoing before subduction of the main continental body (Figure 5b). In the "slow" subduction case of model **7** ($Vx = 0.3$ cm/year), microcontinental upper crust accretes at the boundary between the subducting and upper plates without deep subduction below the overriding continent (Figure 5c).

Even in the absence of external material influx (model **8**; $Vx = 0$ cm/year) an oceanic subduction is quickly initiated because of the gravitational slab-pull force. However, the active subduction continues only until the microcontinent reaches the overriding plate (3 Myr after onset of the experiment). After 10 Myr, the subduction process is stopped and the system can be considered as steady-state (Figure 5d). This implies that an external push and contractional boundary conditions are necessary to sustain ongoing subduction of the oceanic lithosphere and isolated microblock(s) as well as their moving toward the opposite continent, as is the case for the Africa-Eurasia convergence.

4. Discussion

The formation of isolated microcontinental blocks and their subsequent accretion are common in the geologic record. The separation of microcontinents in a purely extensional setting of the passive rifted margins is attributed to a ridge jump toward the continent due to rheological weakening of the passive margin lithosphere resulting from the thermal impact of the mantle plume (Figure 1a). Repeated jumps of mid-oceanic ridges toward nearby hot spots within oceanic lithosphere have been reproduced numerically by Mittelstaedt et al. (2008, 2011) and observed by d'Acremont et al. (2010). In the context of the continental lithosphere, the 2-D thermo-mechanical modeling by Lavecchia et al. (2017) showed an abandonment of the rift initially localized in a preexisting zone of lithospheric weakness and associated rift jump toward the thermally activated mantle plume. Mantle upwelling, thus, was confirmed to be one of the key factors in the contrasting continental rifting characterized by both "passive/amagmatic" and "active/magmatic" branches (see also 3-D experiments by Koptev et al., 2015, 2016; Koptev, Burov, et al., 2018; Koptev, Cloetingh, et al., 2018) that may further evolve into breakup centers embracing isolated continental block (Beniest, Koptev, Leroy, et al., 2017). In analog models, a complete separation of the microcontinental body from a parent continent is also strongly connected to the thermal weakening due to the presence of a hot spot (Dubinin et al., 2018).

Continental microblocks separated from the main body of the African plate during its northward motion toward Eurasia accommodated by uninterrupted oceanic and continental subduction define a second type of microcontinent behavior (Figure 2b). The northern margin of Africa is known to have experienced fragmentation since the Paleozoic when a series of small continental plates have been rifted away from Gondwana (the Avalonia and Armorica terranes in the Ordovician, the European Hunic terranes in the Silurian, and the Cimmerian blocks in the Permian) and subsequently accreted along the active southern margin of Laurussia (Matte, 2001; Stampfli & Borel, 2002; Von Raumer et al., 2003). The European Hunic terranes have been detached from the active northern Gondwana margin by oceanward migration of the arc-trench systems due to slab rollback of the Rheic ocean (Stampfli et al., 2002; Stampfli & Borel, 2002) and thus were bounded by different—active and passive—plate margins. Evolution and possible mechanisms for formation of such back-arc basins separating the volcanic arcs from the mainland have been thoroughly investigated by several numerical studies over the last decade (Clark et al., 2008; Dal Zilio et al., 2018; Gerya & Meilick, 2011; Sizova et al., 2010). In contrast, other continental domains separated from northern Gondwana in the Paleozoic (the Avalonia and Armorica terranes and the Cimmerian blocks) had initially two passive margins (Matte, 2001; Stampfli & Borel, 2002) similar to the Mesozoic Apulian microcontinent segregated from the passive African margin (Jolivet et al., 2016). Formation of these microcontinents with two passive margins but formed on the subducting plate (Figure 1b) is not apparent since they represent the results of extensional processes while developed in an overall context of convergence.

In the 3-D thermo-mechanical numerical results presented here, we combine a preimposed convergence rate with the self-driven dynamics of a mantle plume. The push of the mantle plume impinged at the base

of the African plate triggering local extension is shown to be sufficient for microblock separation. Our results reveal the key role of the initial thermal structure of the overlying continent in this process because continental breakup and microcontinent separation occurs only under condition of a relatively elevated geotherm (see models **4**–**8**; Figures 3d, 4, and 5). In contrast, variations in plume temperature do not appear to be crucial (models **2**–**3**; Figures 3b and 3c). The presence of a continuous external push (possibly resulting from a large-scale mantle flow due to the large plume postulated by Jolivet et al., 2016) is shown to be indispensable to sustain continental subduction of the separated microblock (compare Figures 5a–5c and 5d). In the final stages of the experiments, the subduction of the separated microblock is followed by tectonic exhumation of the upper crust (Figures 5a–5c). This is consistent with continental accretion in the eastern Mediterranean zone during the Cenozoic where it has occurred by decoupling crustal nappes from the subducting continental lithosphere in contrast to the eastern Anatolia characterized by "true" collisional events (Menant et al., 2018).

The thermo-mechanical models presented here consider the mantle plume as a necessary ingredient for the generation of locally extensional tectonics in a regionally compressive environment that ultimately results in microcontinent formation. Note though that we do not rule out other factors possibly contributing to the separation of a microblock from the subducting plate such as (1) regional-scale plate reorganization associated to sharp convergence acceleration (Agard et al., 2006, 2007) or (2) lateral transition from subduction to collision along the convergent boundary (Bellahsen et al., 2003; Dercourt et al., 1993; Koptev, Gerya, et al., 2018) in the presence of (3) preexisting zones of weakness (Dixon et al., 1987; Ligi et al., 2012).

5. Conclusions

The modeling results presented here reveal that even in a convergent tectonic setting, an upwelling flow of hot mantle material can trigger localized extension, rifting, and breakup. This ultimately leads to the opening of a new oceanic basin that separates a microcontinental sliver from the main continent belonging to a subducting lithospheric plate. The scenario evaluated involves plume-induced separation of a microcontinent away from the main continent during uninterrupted subduction. This can be compared to the Paleozoic-Cenozoic evolution of Africa, which is characterized by subsequent separation of several microcontinental pieces while subduction of the oceanic and continental lithosphere below the Eurasian margin was ongoing.

Acknowledgments
We thank two reviewers for their helpful and constructive comments. This study is cofunded by the Advanced ERC grant 290864 RHEOLITH (L. Jolivet–A. Koptev) and ERC Consolidator grant 615703 EXTREME (T. Ehlers–A. Koptev). The numerical simulations were performed on the ERC-funded SGI Ulysse cluster of ISTeP. The computer code I3ELVIS used to generate our 3-D thermo-mechanical numerical model is provided in Gerya (2010). Open source software ParaView (http://www.paraview.org) was used for 3-D visualization. The figures in the supporting information contain the numerical simulation data.

References

Agard, P., Jolivet, L., Vrielynck, B., Burov, E., & Monie, P. (2007). Plate acceleration: The obduction trigger? *Earth and Planetary Science Letters*, *258*(3–4), 428–441. https://doi.org/10.1016/j.epsl.2007.04.002

Agard, P., Monié, P., Gerber, W., Omrani, J., Molinaro, M., Meyer, B., et al. (2006). Transient, synobduction exhumation of Zagros blueschists inferred from P-T, deformation, time, and kinematic constraints: Implications for Neotethyan wedge dynamics. *Journal of Geophysical Research*, *111*, B11401. https://doi.org/10.1029/2005JB004103

Agard, P., Omrani, J., Jolivet, L., Whitechurch, H., Vrielynck, B., Spakman, W., et al. (2011). Zagros orogeny: A subduction-dominated process. *Geological Magazine*, *148*(5–6), 692–725. https://doi.org/10.1017/S001675681100046X

Barrier, E., & Vrielynck, B. (2008). *Paleotectonic maps of the Middle East. Atlas of 14 Maps*. Paris: Middle East Basin Evolution Programme.

Barrier, E., Vrielynck, B., Brouillet, J. F., & Brunet, M. F. (2018). Paleotectonic reconstruction of the Central Tethyan Realm. Tectono-sedimentary-palinspastic maps from Late Permian to Pliocene. *Atlas of 20 maps (scale: 1/15 000 000), CCGM/CGMW*. http://www.ccgm.org.

Bellahsen, N., Faccenna, C., Funiciello, F., Daniel, J. M., & Jolivet, L. (2003). Why did Arabia separate from Africa? Insights from 3-D laboratory experiments. *Earth and Planetary Science Letters*, *216*(3), 365–381. https://doi.org/10.1016/S0012-821X(03)00516-8

Beniest, A., Koptev, A., & Burov, E. (2017). Numerical models for continental break-up: Implications for the South Atlantic. *Earth and Planetary Science Letters*, *461*, 176–189. https://doi.org/10.1016/j.epsl.2016.12.034

Beniest, A., Koptev, A., Leroy, S., Sassi, W., & Guichet, X. (2017). Two-branch break-up systems by a single mantle plume: Insights from numerical modeling. *Geophysical Research Letters*, *44*, 9589–9597. https://doi.org/10.1002/2017GL074866

Blischke, A., Gaina, C., Hopper, J. R., Péron-Pinvidic, G., Brandsdottir, B., Guarnieri, P., et al. (2016). The Jan Mayen microcontinent: An update of its architecture, structural development and role during the transition from the Ægir Ridge to the mid-oceanic Kolbeinsey Ridge. *Geological Society London, Special Publications*, *447*(1), 299–337. https://doi.org/10.1144/SP447.5

Bosworth, W., Huchon, P., & McClay, K. (2005). The Red Sea and Gulf of Aden basins. *Journal of African Earth Sciences*, *43*(1–3), 334–378. https://doi.org/10.1016/j.jafrearsci.2005.07.020

Bruhn, R. L., Pavlis, T. L., Plafker, G., & Serpa, L. (2004). Deformation during terrane accretion in the Saint Elias orogen, Alaska. *Geological Society of America Bulletin*, *116*(7–8), 771–787. https://doi.org/10.1130/B25182.1

Burg, J. P., & Gerya, T. V. (2005). The role of viscous heating in Barrovian metamorphism of collisional orogens: Thermomechanical models and application to the Lepontine Dome in the Central Alps. *Journal of Metamorphic Geology*, *23*(2), 75–95. https://doi.org/10.1111/j.1525-1314.2005.00563.x

Burke, K., Steinberger, B., Torsvik, T. H., & Smethurst, M. A. (2008). Plume generation zones at the margins of large low shear velocity provinces on the core–mantle boundary. *Earth and Planetary Science Letters*, *265*(1–2), 49–60. https://doi.org/10.1016/j.epsl.2007.09.042

Clark, S. R., Stegman, D., & Dietmar, R. M. (2008). Episodicity in back-arc tectonic regimes. *Physics of the Earth and Planetary Interiors*, *171*(1–4), 265–279. https://doi.org/10.1016/j.pepi.2008.04.012

Collier, J. S., Minshull, T. A., Hammond, J. O. S., Whitmarsh, R. B., Kendall, J., Sansom, V., et al. (2009). Factors influencing magmatism during continental breakup: New insights from a wide-angle seismic experiment across the conjugate Seychelles-Indian margins. *Journal of Geophysical Research*, *114*, B03101. https://doi.org/10.1029/2008JB005898

Connolly, J. A. (2005). Computation of phase equilibria by linear programming: A tool for geodynamic modeling and its application to subduction zone decarbonation. *Earth and Planetary Science Letters*, *236*(1–2), 524–541. https://doi.org/10.1016/j.epsl.2005.04.033

Crameri, F., Schmeling, H., Golabek, G. J., Duretz, T., Orendt, R., Buiter, S. J. H., et al. (2012). A comparison of numerical surface topography calculations in geodynamic modelling: An evolution of the "sticky air" method. *Geophysical Journal International*, *189*(1), 38–54. https://doi.org/10.1111/j.1365-246X.2012.05388.x

d'Acremont, E., Leroy, S., Maia, M., Gente, P., & Autin, J. (2010). Volcanism, jump and propagation on the Sheba ridge, eastern Gulf of Aden: Segmentation evolution and implications for oceanic accretion processes. *Geophysical Journal International*, *180*(2), 535–551. https://doi.org/10.1111/j.1365-246X.2009.04448.x

Dal Zilio, L. (2018). Subduction-driven Earth machine. *Nature Geoscience*, *11*(4), 229. https://doi.org/10.1038/s41561-018-0102-z

Dal Zilio, L., Faccenda, M., & Capitanio, F. (2018). The role of deep subduction in supercontinent breakup. *Tectonophysics*, *746*, 312–324. https://doi.org/10.1016/j.tecto.2017.03.006

Deevsalar, R., Shinjo, R., Liégeois, J. P., Valizadeh, M. V., Ahmadian, J., Yeganehfar, H., et al. (2018). Subduction-related mafic to felsic magmatism in the Malayer-Boroujerd plutonic complex, western Iran. *Swiss Journal of Geosciences*, *111*(1-2), 269–293. https://doi.org/10.1007/s00015-017-0287-y

Dercourt, J., Ricou, L. E., & Vrielynck, B. (1993). *Atlas Tethys palaeoenvironmental maps*. Paris: BEICIP-FRANLAB Gauthier-Vollars.

Dercourt, J., Zonenshain, L. P., Ricou, L.-E., Kazmin, V. G., Le Pichon, X., Knipper, A. L., et al. (1986). Geological evolution of the Tethys belt from the Atlantic to the Pamirs since the Lias. *Tectonophysics*, *123*(1–4), 241–315. https://doi.org/10.1016/0040-1951(86)90199-X

Dickin, A. P., Fallick, A. E., Halliday, A. N., Macintyre, R. M., & Stephens, W. E. (1986). An isotopic and geochronological investigation of the younger igneous rocks of the Seychelles microcontinent. *Earth and Planetary Science Letters*, *81*(1), 46–56. https://doi.org/10.1016/0012-821X(86)90099-3

Dixon, T. H., Stern, R. J., & Hussein, I. M. (1987). Control of Red Sea rift geometry by Precambrian structures. *Tectonics*, *6*(5), 551–571. https://doi.org/10.1029/TC006i005p00551

Dubinin, E. P., Grokholsky, A. L., & Makushkina, A. I. (2018). Physical modeling of the formation conditions of microcontinents and continental marginal plateaus. *Izvestiya, Physics of the Solid Earth*, *54*(1), 66–78. https://doi.org/10.1134/S1069351318010056

Duretz, T., May, D. A., Gerya, T. V., & Tackley, P. J. (2011). Discretization errors and free surface stabilization in the finite difference and marker-in-cell method for applied geodynamics: A numerical study. *Geochemistry, Geophysics, Geosystems*, *12*, Q07004. https://doi.org/10.1029/2011GC003567

Enkelmann, E., Piestrzeniewicz, A., Falkowski, S., Stübner, K., & Ehlers, T. A. (2017). Thermochronology in southeast Alaska and southwest Yukon: Implications for North American Plate response to terrane accretion. *Earth and Planetary Science Letters*, *457*, 348–358. https://doi.org/10.1016/j.epsl.2016.10.032

Ernst, R. E. (2014). *Large igneous provinces*, (p. 653). Cambridge, UK: Cambridge University Press.

Exon, N. F., Berry, R. F., Crawford, A. J., & Hill, P. J. (1997). Geological evolution of the East Tasman Plateau, a continental fragment southeast of Tasmania. *Australian Journal of Earth Sciences*, *44*(5), 597–608. https://doi.org/10.1080/08120099708728339

Faccenna, C., Becker, T. W., Jolivet, L., & Keskin, M. (2013). Mantle convection in the Middle East: Reconciling Afar upwelling, Arabia indentation and Aegean trench rollback. *Earth and Planetary Science Letters*, *375*, 254–269. https://doi.org/10.1016/j.epsl.2013.05.043

Forte, A. M., & Mitrovica, J. X. (2001). Deep-mantle high-viscosity flow and thermochemical structure inferred from seismic and geodynamic data. *Nature*, *410*(6832), 1049–1056. https://doi.org/10.1038/35074000

Frizon de Lamotte, D., Raulin, C., Mouchot, N., Christophe, J., Daveau, W., Blanpied, C., & Ringenbach, J. C. (2011). The southernmost margin of the Tethys realm during the Mesozoic and Cenozoic: Initial geometry and timing of the inversion processes. *Tectonics*, *30*, TC3002. https://doi.org/10.1029/2010TC002691

Gaina, C., Gernigon, L., & Ball, P. (2009). Palaeocene—Recent plate boundaries in the NE Atlantic and the formation of the Jan Mayen microcontinent. *Journal of the Geological Society*, *166*(4), 601–616. https://doi.org/10.1144/0016-76492008-112

Gaina, C., Müller, R. D., Brown, B., & Ishihara, T. (2003). Microcontinent formation around Australia. *Geological Society of America Special Paper*, *372*, 405–416. https://doi.org/10.1111/j.1365-246X.2007.03450.x

Gaina, C., Roest, W. R., Müller, R. D., & Symonds, P. (1998). The opening of the Tasman Sea: A gravity anomaly animation. *Earth Interactions*, *2*(4), 1–23. https://doi.org/10.1175/1087-3562(1998)002<0001:TOOTTS>2.3.CO;2

Ganerød, M., Torsvik, T. H., Van Hinsbergen, D. J. J., Gaina, C., Cordu, F., Werner, S., et al. (2011). Palaeoposition of the Seychelles microcontinent in relation to the Deccan Traps and the Plume Generation Zone in Late Cretaceous-Early Palaeogene time. *Geological Society London, Special Publication*, *357*(1), 229–252. https://doi.org/10.1144/SP357.12

Gerya, T. V. (2010). *Introduction to numerical geodynamic modelling*, (p. 345). Cambridge, UK: Cambridge University Press.

Gerya, T. V. (2013). Initiation of transform faults at rifted continental margins: 3D petrological-thermomechanical modeling and comparison to the Woodlark Basin. *Petrology*, *21*(6), 550–560. https://doi.org/10.1134/S0869591113060039

Gerya, T. V., & Meilick, F. I. (2011). Geodynamic regimes of subduction under an active margin: Effects of rheological weakening by fluids and melts. *Journal of Metamorphic Geology*, *29*(1), 7–31. https://doi.org/10.1111/j.1525-1314.2010.00904.x

Gerya, T. V., & Yuen, D. A. (2007). Robust characteristics method for modelling multiphase visco-elasto-plastic thermo-mechanical problems. *Physics of the Earth and Planetary Interiors*, *163*(1–4), 83–105. https://doi.org/10.1016/j.pepi.2007.04.015

Ghebreab, W. (1998). Tectonics of the Red Sea region reassessed. *Earth-Science Reviews*, *45*(1–2), 1–44. https://doi.org/10.1016/S0012-8252(98)00036-1

Gudlaugsson, S. T., Gunnarsson, K., Sand, M., & Skogseid, J. (1988). Tectonic and volcanic events at the Jan Mayen Ridge microcontinent. *Geological Society London, Special Publication*, *39*(1), 85–93. https://doi.org/10.1144/GSL.SP.1988.039.01.09

Gurnis, M., Mitrovica, J. X., Ritsema, J., & van Heijst, H. J. (2000). Constraining mantle density structure using geological evidence of surface uplift rates: The case of the African superplume. *Geochemistry, Geophysics, Geosystems*, *1*(7), 1020. https://doi.org/10.1029/1999GC000035

Hafkenscheid, E., Wortel, M. J. R., & Spakman, W. (2006). Subduction history of the Tethyan region derived from seismic tomography and tectonic reconstructions. *Journal of Geophysical Research*, *111*, B08401. https://doi.org/10.1029/2005JB003791

Heron, P. J., Lowman, J. P., & Stein, C. (2015). Influences on the positioning of mantle plumes following supercontinent formation. *Journal of Geophysical Research: Solid Earth*, *120*, 3628–3648. https://doi.org/10.1002/2014JB011727

Joffe, S. A. M., & Garfunkel, Z. V. I. (1987). Plate kinematics of the circum Red Sea—A re-evaluation. *Tectonophysics*, *141*(1–2), 5–22. https://doi.org/10.1016/0040-1951(87)90171-5

Jolivet, L., & Faccenna, C. (2000). Mediterranean extension and the Africa-Eurasia collision. *Tectonics*, *19*(6), 1095–1106. https://doi.org/10.1029/2000TC900018

Jolivet, L., Faccenna, C., Agard, P., Frizon De Lamotte, D., Menant, A., Sternai, P., & Guillocheau, F. (2016). Neo-Tethys geodynamics and mantle convection: From extension to compression in Africa and a conceptual model for obduction. *Canadian Journal of Earth Sciences*, *53*(11), 1–15. https://doi.org/10.1139/cjes-2015-0118

Jolivet, L., Faccenna, C., Goffe, B., Burov, E., & Agard, P. (2003). Subduction tectonics and exhumation of high-pressure metamorphic rocks in the Mediterranean orogens. *American Journal of Science*, *303*(5), 353–409. https://doi.org/10.2475/ajs.303.5.353

Jourdan, F., Féraud, G., Bertrand, H., Watkeys, M. K., & Renne, A. P. (2008). The 40Ar/39Ar ages of the sill complex of the Karoo large igneous province: Implications for the Pliensbachian-Toarcian climate change. *Geochemistry, Geophysics, Geosystems*, *9*, Q06009. https://doi.org/10.1029/2008GC001994

Katz, R. F., Spiegelman, M., & Langmuir, C. H. (2003). A new parameterization of hydrous mantle melting. *Geochemistry, Geophysics, Geosystems*, *4*(9), 1073. https://doi.org/10.1029/2002GC000433

Koptev, A., Burov, E., Calais, E., Leroy, S., Gerya, T., Guillou-Frottier, L., & Cloetingh, S. (2016). Contrasted continental rifting via plume-craton interaction: Applications to Central East African Rift. *Geoscience Frontiers*, *7*(2), 221–236. https://doi.org/10.1016/j.gsf.2015.11.002

Koptev, A., Burov, E., Gerya, T., Le Pourhiet, L., Leroy, S., Calais, E., & Jolivet, L. (2018). Plume-induced continental rifting and break-up in ultra-slow extension context: Insights from 3D numerical modeling. *Tectonophysics*, *746*, 121–137. https://doi.org/10.1016/j.tecto.2017.03.025

Koptev, A., Calais, E., Burov, E., Leroy, S., & Gerya, T. (2015). Dual continental rift systems generated by plume-lithosphere interaction. *Nature Geoscience*, *8*(5), 388–392. https://doi.org/10.1038/NGEO2401

Koptev, A., Cloetingh, S., Gerya, T., Calais, E., & Leroy, S. (2018). Non-uniform splitting of a single mantle plume by double cratonic roots: Insight into the origin of the central and southern East African Rift System. *Terra Nova*, *30*(2), 125–134. https://doi.org/10.1111/ter.12317

Koptev, A., Gerya, T., Calais, E., Leroy, S., & Burov, E. (2018). Afar triple junction triggered by plume-assisted bi-directional continental break-up. *Scientific Reports*, *8*(1), 14742. https://doi.org/10.1038/s41598-018-33117-3

Lavecchia, A., Thieulot, C., Beekman, F., Cloetingh, S., & Clark, S. (2017). Lithosphere erosion and continental breakup: Interaction of extension, plume upwelling and melting. *Earth and Planetary Science Letters*, *467*, 89–98. https://doi.org/10.1016/j.epsl.2017.03.028

Leroy, S., d'Acremont, E., Tiberi, C., Basuyau, C., Autin, J., Lucazeau, F., & Sloan, H. (2010). Recent off-axis volcanism in the eastern Gulf of Aden: Implications for plume-ridge interaction. *Earth and Planetary Science Letters*, *293*(1–2), 140–153. https://doi.org/10.1016/j.epsl.2010.02.036

Leroy, S., Razin, P., Autin, J., Bache, F., D'Acremont, E., Watremez, L., et al. (2012). From rifting to oceanic spreading in the Gulf of Aden: A synthesis. *Arabian Journal of Geosciences*, *5*(5), 859–901. https://doi.org/10.1007/s12517-011-0475-4

Ligi, M., Bonatti, E., Bortoluzzi, G., Cipriani, A., Cocchi, L., Caratori Tontini, F., et al. (2012). Birth of an ocean in the Red Sea: Initial pangs. *Geochemistry, Geophysics, Geosystems*, *13*, Q08009. https://doi.org/10.1029/2012GC004155

Lundin, E., & Doré, A. G. (2002). Mid-Cenozoic post-breakup deformation in the 'passive' margins bordering the Norwegian-Greenland Sea. *Marine and Petroleum Geology*, *19*(1), 79–93. https://doi.org/10.1016/S0264-8172(01)00046-0

Matte, P. (2001). The Variscan collage and orogeny (480 ± 290 Ma) and the tectonic definition of the Armorica microplate: a review. *Terra Nova*, *13*(2), 122–128. https://doi.org/10.1046/j.1365-3121.2001.00327.x

Menant, A., Jolivet, L., Tuduri, J., Loiselet, C., Bertrand, G., & Guillou-Frottier, L. (2018). 3D subduction dynamics: A first-order parameter of the transition from copper- to gold-rich deposits in the eastern Mediterranean region. *Ore Geology Reviews*, *94*, 118–135. https://doi.org/10.1016/j.oregeorev.2018.01.023

Menant, A., Jolivet, L., & Vrielynck, B. (2016). Kinematic reconstructions and magmatic evolution illuminating crustal and mantle dynamics of the eastern Mediterranean region since the late Cretaceous. *Tectonophysics*, *675*, 103–140. https://doi.org/10.1016/j.tecto.2016.03.007

Mittelstaedt, E., Ito, G., & Behn, M. D. (2008). Mid-ocean ridge jumps associated with hotspot magmatism. *Earth and Planetary Science Letters*, *266*(3–4), 256–270. https://doi.org/10.1016/j.epsl.2007.10.055

Mittelstaedt, E., Ito, G., & van Hunen, J. (2011). Repeat ridge jumps associated with plume-ridge interaction, melt transport and ridge migration. *Journal of Geophysical Research*, *116*, B01102. https://doi.org/10.1029/2010JB007504

Mohriak, W. U., & Leroy, S. (2013). Architecture of rifted continental margins and break-up evolution: Insights from the South Atlantic, North Atlantic and Red Sea-Gulf of Aden conjugate margins. *Geological Society London, Special Publications*, *369*, SP369–17(1), 497–535. https://doi.org/10.1144/SP369.17

Molnar, N. E., Cruden, A. R., & Betts, P. G. (2018). Unzipping continents and the birth of microcontinents. *Geology*, *46*(5), 451–454. https://doi.org/10.1016/j.earscirev.2010.01.002.2

Müller, R. D., Gaina, C., Roest, W., & Hansen, D. L. (2001). A recipe for microcontinent formation. *Geology*, *29*(3), 203–206. https://doi.org/10.1130/0091-7613(2001)029<0203:ARFMF>2.0.CO;2

Myhre, A. M., Eldholm, O., & Sundvor, E. (1984). The Jan Mayen Ridge: Present status. *Polar Research*, *2*(1), 47–59. https://doi.org/10.1111/j.1751-8369.1984.tb00485.x

Peron-Pinvidic, G., Gernigon, L., Gaina, C., & Ball, P. (2012). Insights from the Jan Mayen system in the Norwegian-Greenland sea—I. Mapping of a microcontinent. *Geophysical Journal International*, *191*(2), 413–435. https://doi.org/10.1111/j.1365-246X.2012.05639.x

Peron-Pinvidic, G., & Manatschal, G. (2010). From microcontinents to extensional allochthons: Witnesses of how continents rift and break apart? *Petroleum Geoscience*, *16*(3), 189–197. https://doi.org/10.1144/1354-079309-903

Plafker, G., & Berg, H. C. (1994). *Overview of the geology and tectonic evolution of Alaska* (pp. 989–1021). Boulder, CO: The Geology of Alaska*:* Geological Society of America.

Plummer, P. S., & Belle, E. R. (1995). Mesozoic tectono-stratigraphic evolution of the Seychelles microcontinent. *Sedimentary Geology*, *96*(1–2), 73–91. https://doi.org/10.1016/0037-0738(94)00127-G

Ricou, L. E. (1994). Tethys reconstructed: Plates, continental fragments and their boundaries since 260 Ma from Central America to South-eastern Asia. *Geodinamica Acta*, *7*(4), 169–218. https://doi.org/10.1080/09853111.1994.11105266

Ritsema, J., van Heijst, H. J., & Woodhouse, J. H. (1999). Complex shear wave velocity structure imaged beneath Africa and Iceland. *Science*, *286*(5446), 1925–1928. https://doi.org/10.1126/science.286.5446.1925

Roger, J., Platel, J. P., Cavelier, C., & Bourdillon-de-Grisac, C. (1989). Données nouvelles sur la stratigraphie et l'histoire géologique du Dhofar (Sultanat d'Oman). *Bulletin de La Société Géologique de France*, *2*, 265–277. https://doi.org/10.2113/gssgfbull

Schiffer, C., Peace, A., Phethean, J., Gernigon, L., McCaffrey, K., Petersen, K. D., & Foulger, G. (2018). The Jan Mayen microplate complex and the Wilson cycle. *Geological Society London, Special Publication*, *470*, SP470–2. https://doi.org/10.1144/SP470.2

Scrutton, R. A. (1976). Microcontinents and their significance. *Geodynamics: Progress and Prospects*, *5*, 177–189.

Sengör, A. M. C., & Yilmaz, Y. (1981). Tethyan evolution of Turkey: A plate tectonic approach. *Tectonophysics*, *75*(3–4), 181–241. https://doi.org/10.1016/0040-1951(81)90275-4

Sizova, E., Gerya, T., Brown, M., & Perchuk, L. L. (2010). Subduction styles in the Precambrian: Insight from numerical experiments. *Lithos*, *116*(3–4), 209–229. https://doi.org/10.1016/j.lithos.2009.05.028

Stampfli, G. M., & Borel, G. D. (2002). A plate tectonic model for the Paleozoic and Mesozoic constrained by dynamic plate boundaries and restored synthetic oceanic isochrons. *Earth and Planetary Science Letters*, *196*(1), 17–33. https://doi.org/10.1016/S0012-821X(01)00588-X

Stampfli, G. M., Von Raumer, J. F., & Borel, G. D. (2002). Paleozoic evolution of pre-Variscan terranes: From Gondwana to the Variscan collision. *Geological Society of America Special Paper*, *364*, 263–280.

Takin, M. (1972). Iranian geology and continental drift in the Middle East. *Nature*, *235*(5334), 147–150. https://doi.org/10.1038/235147a0

Torsvik, T. H., Amundsen, H. E. F., Trønnes, R. G., Doubrovine, P. V., Gaina, C., Kusznir, N. J., et al. (2015). Continental crust beneath southeast Iceland. *Proceedings of the National Academy of Sciences*, *112*(15), E1818–E1827. https://doi.org/10.1073/pnas.1423099112

Torsvik, T. H., Smethurst, M. A., Burke, K., & Steinberger, B. (2006). Large igneous provinces generated from the margins of the large low-velocity provinces in the deep mantle. *Geophysical Journal International*, *167*(3), 1447–1460. https://doi.org/10.1111/j.1365-246X.2006.03158.x

Turcotte, D. L., & Schubert, G. (2002). *Geodynamics*, (p. 456). Cambridge, UK: Cambridge University Press.

Van Hinsbergen, D. J. J., Langereis, C. G., & Meulenkamp, J. E. (2005). Revision of the timing, magnitude and distribution of Neogene rotations in the western Aegean region. *Tectonophysics*, *396*(1–2), 1–34. https://doi.org/10.1016/j.tecto.2004.10.001

Van Staal, C. R., Barr, S. M., & Percival, J. A. (2012). Lithospheric architecture and tectonic evolution of the Canadian Appalachians and associated Atlantic margin. In J. A. Percival, F. A. Cook, & R. M. Clowes (Eds.), *Tectonic styles in Canada: The LITHOPROBE perspective*, (Vol. 49, pp. 41–95). St. John's, Newfoundland, Canada: Geological Association of Canada, Special Paper.

Van Staal, C. R., Whalen, J. B., Valverde-Vaquero, P., Zagorevski, A., & Rogers, N. (2009). Pre-Carboniferous, episodic accretion-related, orogenesis along the Laurentian margin of the northern Appalachians. *Geological Society, London, Special Publications*, *327*(1), 271–316. https://doi.org/10.1144/SP327.13

Vink, E., Morgen, J. M., & Zhao, W.-L. (1984). Preferential rifting of continents: A source of displaced terranes. *Journal of Geophysical Research*, *89*(B12), 10,072–10,076. https://doi.org/10.1029/JB089iB12p10072

Vogt, K., Matenco, L., & Cloetingh, S. (2017). Crustal mechanics control the geometry of mountain belts. Insights from numerical modelling. *Earth and Planetary Science Letters*, *460*, 12–21. https://doi.org/10.1016/j.epsl.2016.11.016

Vogt, K., Willingshofer, E., Matenco, L., Sokoutis, D., Gerya, T., & Cloetingh, S. (2018). The role of lateral strength contrasts in orogenesis: A 2D numerical study. *Tectonophysics*, *476*, 549–561. https://doi.org/10.1016/j.tecto.2017.08.010

Von Raumer, J. F., Stampfli, G. M., & Bussy, F. (2003). Gondwana-derived microcontinents—The constituents of the Variscan and Alpine collisional orogens. *Tectonophysics*, *365*(1–4), 7–22. https://doi.org/10.1016/S0040-1951(03)00015-5

Watchorn, F., Nichols, G. J., & Bosence, D. W. J. (1998). *Rift-related sedimentation and stratigraphy, southern Yemen (Gulf of Aden). In Sedimentation and Tectonics in Rift Basins Red Sea:-Gulf of Aden* (pp. 165–189). Dordrecht: Springer. https://doi.org/10.1007/978-94-011-4930-3_11

Whittaker, J. M., Williams, S. E., Halpin, J. A., Wild, T. J., Stilwell, J. D., Jourdan, F., & Daczko, N. R. (2016). Eastern Indian Ocean microcontinent formation driven by plate motion changes. *Earth and Planetary Science Letters*, *454*, 203–212. https://doi.org/10.1016/j.epsl.2016.09.019

Willingshofer, E., Sokoutis, D., Luth, S. W., Beekman, F., & Cloetingh, S. (2013). Subduction and deformation of the continental lithosphere in response to plate and crust-mantle coupling. *Geology*, *41*(12), 1239–1242. https://doi.org/10.1130/G34815.1

Zhang, N., Zhong, S., Leng, W., & Li, Z. X. (2010). A model for the evolution of the Earth's mantle structure since the Early Paleozoic. *Journal of Geophysical Research*, *115*, B06401. https://doi.org/10.1029/2009JB006896